Since January 2020 Elsevier has created a COVID-19 resource centre with free information in English and Mandarin on the novel coronavirus COVID-19. The COVID-19 resource centre is hosted on Elsevier Connect, the company's public news and information website.

Journal of Molecular Structure 1219 (2020) 128610

Contents lists available at ScienceDirect

Journal of Molecular Structure

journal homepage: http://www.elsevier.com/locate/molstruc

Experimental isolation and spectroscopic characterization of squamocin acetogenin combining FT-IR, FT-Raman and UV−Vis spectra with DFT calculations

José Ruiz Hidalgo [a], Adriana Neske [a], Maximiliano A. Iramain [b], Patricia E. Alvarez [c], Patricio Leyton Bongiorno [d, e], Silvia Antonia Brandán [b, *]

[a] UNT-FBQF-Argentina, Instituto de Química Orgánica, Tucumán, Argentina
[b] Cátedra de Química General, Instituto de Química Inorgánica, Facultad de Bioquímica, Química y Farmacia, Universidad Nacional de Tucumán, Ayacucho 471, 4000, San Miguel de Tucumán, Tucumán, Argentina
[c] Cátedra Física I, Instituto de Física, Facultad de Bioquímica, Química y Farmacia. Universidad Nacional de Tucumán, Ayacucho 471, 4000, S. M. de Tucumán, Argentina
[d] Laboratorio de Fotofísica y Espectroscopia Molecular N°401, Av. Universidad #330, Campus Curauma, Valparaíso, Chile
[e] Pontificia Universidad Católica de Valparaíso, Chile

ARTICLE INFO

Article history:
Received 27 April 2020
Received in revised form
2 June 2020
Accepted 3 June 2020
Available online 8 June 2020

Keywords:
Acetogenin
Molecular structure
Squamocin
DFT calculations
Vibrational spectra

ABSTRACT

Squamocin, an annonaceous acetogenin has been experimentally isolated and characterized in the solid state using the FT-IR and FT-Raman spectra and in methanol solution by UV−visible spectrum. The main bands observed were assigned combining the IR and Raman spectra with hybrid functional B3LYP/6-31G* calculations. Structural, electronic and topological properties were predicted at the same level of theory for the most stable conformer of squamocin in gas phase and methanol solution. A corrected solvation energy value of −147.54 kJ/mol was predicted for squamocin in methanol while the atomic population natural (NPA) charges evidence higher values on O atoms of R2 and R3 rings, as compared with the corresponding to lactone ring. Mapped MEP surfaces suggest that nucleophilic regions are located on the O atoms of three rings and of OH bonds belonging to side chain, in agreement with the higher charges values evidenced on these O atoms while electrophilic regions are predicted on the H atoms of OH groups. High stabilities of squamocin in both media was revealed by AIM studies while only in methanol solution by NBO calculations. The expansion of volume and the higher dipole moment in methanol suggest a clear solvation of squamocin by solvent molecules. Gap values have evidenced that squamocin is most reactive in methanol while that its large aliphatic chain produces an increases the reactivity of this γ-lactone, as compared with ascorbic acid lactone. Reasonable concordances among the predicted UV−visible and IR, Raman spectra with the corresponding experimental ones were found.

1. Introduction

Squamocin is an annonaceous acetogenin (ACG) in whose structure there are a large side chain of CH_2 groups with bis-tetrahydrofuranic (bis-THF) rings [1−11]. Isolation of these ACGs was described by Barrachina et al. [2] from the methanolic extract of *Annona cherimolia* seeds. Antimicrobial and cytotoxic activities were reported for squamocin [1,2,4,5,8−10] while other ACGs were estimated by structure-activity relationships against human tumor cells [3,7,11]. On the other hand, motrilin, an acetogenin similar to squamocin, have been evaluated as corrosion inhibitors for carbon steel in acidic solutions [12] and its structural, electronic and topological properties were recently studied together with its vibrational and ultraviolet−visible spectra [13]. In this work, we have studied the properties of other ACG isolated from *Annona cherimolia* structurally similar to motrilin, named squamocin, however, they differ in the position of the OH group linked to the sides chains, being -$(CH_2)_5$-CH_3 in squamocin and −$(CH_2)_4$−CH_3 in motrilin. In this work, the experimental FT-IR and FT-Raman of squamocin in the solid state and its ultraviolet−visible spectra in methanol solution were reported for first time together with the structural, electronic, topological and vibrational properties. Hence,

* Corresponding author.
E-mail address: sbrandan@fbqf.unt.edu.ar (S.A. Brandán).

https://doi.org/10.1016/j.molstruc.2020.128610
0022-2860/

the aims of this work are the optimizations of squamocin in gas phase and in methanol solution by using hybrid functional B3LYP/6-31G* method [14,15]. After that, the atomic charges, molecular electrostatic potentials, bond orders, donor-acceptor interaction energies and, topological properties are predicted at the same level of theory. Later, the main bands observed in infrared and Raman spectra are assigned by comparison between the corresponding predicted at the same level of theory with the corresponding experimental ones. Besides, the predictions of reactivities and behaviors of squamocin in the two media by using the frontier orbitals and some global descriptors are the great interest taking into account the antimicrobial and cytotoxic activities that present these ACGs [13,16–21]. Finally, the properties obtained for squamocin are compared with those reported for motrilin and for other molecules containing similar groups [13,16–21]. These studies were carried out with the hybrid B3LYP/6-31G* method due to that the squamocin structure presents 109 atoms and, for these reasons, the assignments of main vibrational normal modes of squamocin were performed by comparisons with assignments reported for species containing similar groups [13,18–22]. Predicted ultraviolet–visible spectrum was compared with the corresponding experimental ones in methanol solution, recorded in the same medium at room temperature. The predicted UV-V, FT-IR and FT-Raman spectra have showed good correlations when they are compared with experimental ones.

2. Experimental

2.1. Isolation

Squamocin, an ACG with adjacent bis-THF with OH groups flanking the THF, was isolated by column chromatography on silica gel 60H (5–40 μm, 7336 Merck). The evolution of column chromatography was monitored by thin layer chromatography (TLC). To perform this procedure, Merck F254 chromatofolios were used [10]. Semi preparative HPLC was carried out on a LiChroCartR 100 RP-18 column (25 × 1 cm i. d., 10 μm particle size), flow rate 1.8 mL/min, using MeOH–H_2O 10%.

2.2. Characterization techniques

FT-IR, FT-Raman and UV-V spectroscopies were used to characterize squamocin. A PerkinElmer GX equipment provided with a DTGS detector purged with dry air was employed to record the FT-IR spectrum between 4000 and 400 cm^{-1} with a total of 256 scans and a resolution of 1 cm^{-1}. The FT-Raman spectrum was recorded at room temperature in a 3500-50 cm^{-1} range with a resolution of 4 cm^{-1} and 300 scans by using a Thermo Scientific, DRX Raman Microscope equipped with a laser (excitation line of 1532 nm, 10 mW of laser power). The UV–visible spectrum of the sample was recorded in a 1 mm path length quartz cuvette with methanol at a concentration of 0.1–0.3 mg/mL using a Shimadzu UV–Vis160 A spectrometer.

3. Computational details

The *GaussView* program [22] was employed to model squamocin while its optimizations in gas phase and in methanol solution were performed with the Revision A.02 of Gaussian 09 program [23] by using the hybrid functional B3LYP/6-31G* [14,15]. The 6-31G* basis set was employed in all calculations due to the large aliphatic side chain that presents this molecule. At this level of calculation, only three stable structures for squamocin were observed in the potential energy surface (PES) and only one of them presents global minimum. The most stable structure of squamocin in methanol solution was optimized with the integral equation formalism variant polarised continuum method (IEFPCM) while the solvation energy in the same medium was predicted by using the universal solvation model [24–26]. The solvation energy was corrected by zero point vibrational energy (ZPVE) in addition to non-electrostatic terms. Properties only for some atoms belonging to lactone and furan rings and OH groups of the most stable conformation of squamocin were studied. Besides, the atomic Merz-Singh-Kollman scheme (MK) [27] together with the versions 3.1 and 2000 of NBO and AIM programs [28–30], respectively were employed to calculate natural population charges (NPA), molecular electrostatic potentials (MEP), mains donor-acceptor energy interactions and topological properties in gas phase and in methanol solution. Then, the *GaussView* program [22] was used as an important aid to perform the assignments of the mains bands observed in the vibrational spectra of squamocin. Time-dependent DFT calculations (TD-DFT) by using NStates = 10 at the 6-31G* level of theory with the Revision A.02 of Gaussian 09 program were performed in order to predict the ultraviolet–visible spectrum of squamocin in aqueous solution [23]. Moreover, the frontier orbitals were calculated to obtain the gap values [16,17] and with these parameters the chemical potential (μ), electronegativity (χ), global hardness (η), global softness (S), global electrophilicity index (ω) and nucleophilicity indexes (E) descriptors were computed to predict the reactivities and behaviour of squamocin [18–21]. Then, comparisons of properties predicted for squamocin with those reported for motrilin ACG and other similar species were performed [13,18–21,31,32].

4. Results and discussion

4.1. Structural studies in gas phase and methanol solution

In Fig. 1 is presented the PES as function of the dihedral O45–C44–C37–O34 angle between the two R2 and R3 rings while in Fig. 2 can be seen the most stable structure of squamocin together with the identifications of dihedral O45–C44–C37–O34 angle, its three rings and the atoms numberings only for some simplified fragments indicated by red circles. Clearly, the lactone ring is identified as R1 and the other two as R2 and R3, respectively. In Table 1 are summarized the results of hybrid B3LYP/6-31G* calculations for squamocin ACG in gas phase and in methanol

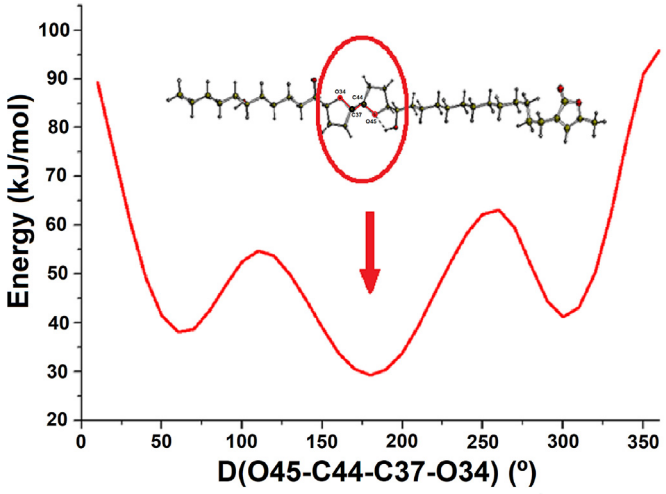

Fig. 1. Potential energy surface (PES) studied for variations of the dihedral O–C–C–O angles for squamocin by using B3LYP/6-31G* method.

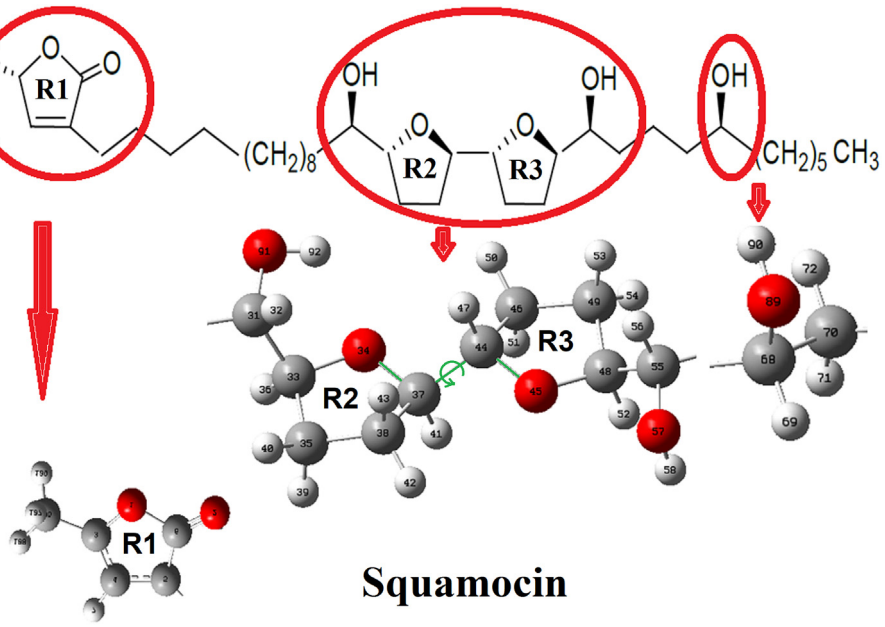

Fig. 2. Theoretical molecular structure of the most stable conformer of squamocin and atoms numbering.

Table 1
Calculated corrected by zero point vibrational energy (ZPVE) and uncorrected energy total (*E*), dipolar moment (μ) and volume (V) values for squamocin acetogenin in gas phase and methanol solution by using B3LYP/6-31G*method. Corrected by ZPVE and by total non-electrostatic terms ($\Delta G_{c/ZPVE}$) and uncorrected by ZPVE solvation energies (ΔG_c) are also presented.

B3LYP/6-31G* Method[a]				
Medium	E (Hartrees)	E_{ZPVE} (Hartrees)	μ (D)	V (Å^3)
GAS	−1975.6402	−1974.6556	6.77	741.8
PCM	−1975.7044	−1974.7208	9.22	752.7
Methanol solution (kJ/mol)				
ΔGun#	ΔGne	ΔGc	ΔGc/ZPVE	ΔV (Å3)
−168.40	−23.07	−145.33	−147.95	10.9

ΔGun# = uncorrected solvation energy, ΔGne = total non electrostatic terms, ΔGc = corrected solvation energies.
[a] This work.

solution [14,15]. Hence, calculated total energy corrected and uncorrected by zero point vibrational energy (ZPVE), dipolar moment and volume values for squamocin acetogenin in the two media together with the corrected and uncorrected solvation energies by the total non-electrostatic terms are also presented in that table. Volumes in both media were computed with the Moldraw program [33]. The dipole moment value of squamocin slightly increases in methanol solution showing a clear expansion of volume (10.9 Å^3) although changes in the directions and orientations of dipole moment vector in solution are not observed, as can be seen in Fig. S1. The corrected solvation energy only by the total non-electrostatic terms reveals a value in methanol solution of −145.33 kJ/mol while when the value is also corrected by ZPVΔE ($G_{c/ZPVE}$) the value increase at −147.95 kJ/mol, a value higher than that observed for morphine hydrochloride (−144.74 kJ/mol) and lower than the value reported for heroin (−161.94 kJ/mol) [34,35]. Here a very important result is that the different positions of the -$(CH_2)_5$-CH_3 and −$(CH_2)_4$−CH_3 groups in the large side chain have few influence on solvation energy value because heroin is different from morphine in two acetyl groups which increase in notable form its solubility and, henec, its solvation energy. At the moment, the experimental structure of squamocin has not been reported and, for this reason, some calculated geometrical parameters in both media have been compared with the experimental values determined for the ascorbic acid (AA) [36,37], as can be seen in Table 2. This comparison is posssible because the R1 ring of squamocin ACG is similar to lactone ring of ascorbic acid. Calculated root-mean-square deviation (RMSD) values were used to compare both structures and the results are also presented in Table 2. Then, the reasonably low RMSD values calculated, which are between 0.053 and 0.048 Å for bond lengths and in 1.6° for bond angles, show very good correlations in the geometrical parameters predicted for squamocin in both media. Now, when the predicted bond C3−O1−C6 angles that belong to lactone ring of squamocin in both media are compared with the corresponding to ring of ascorbic acid (109.1°) we observed a sligth understimation in both values (107.4°). In this squamocin acetogenin, it is observed same signs for the dihedral O34−C37−C44−O45 angle in both media, a resulted different from motrilin acetogenin which evidence a notable change of sign, from positive in gas phase to negative in methanol solution [13].

4.2. Atomic charges and molecular electrostatic potentials (MEP) studies

The presence in squamocin of H bonds donors (three OH groups) and acceptors (seven O atoms) confers at it interesting potential biological and pharmacological properties and, therefore, are of

Table 2
Calculated geometrical parameters for squamocin acetogenin in gas phase and methanol solution compared with the experimental ones for ascorbic acid.

B3LYP/6-31G* Method[a]			Exp[b]
Parameters	Gas	PCM	
Bond lengths (Å)			
R1			
C6═O2	1.213	1.225	1.216
C3—O1	1.357	1.370	1.355
C6—O1	1.424	1.409	1.444
R2			
C33—O34	1.448	1.453	1.355
C37—O34	1.435	1.445	1.444
C44—C37	1.524	1.525	
R3			
C48—O45	1.436	1.449	1.355
C44—O45	1.433	1.442	1.444
C31—O91	1.421	1.434	
C55—O57	1.426	1.437	
C68—O89	1.433	1.442	
RMSD	**0.048**	**0.053**	
Bond angles (°)			
C3—O1—C6	107.4	107.4	109.1
C33—O34—C37	110.8	110.9	
C44—O45—C48	111.0	110.8	
RMSD	**1.6**	**1.6**	
Dihedral angles (°)			
O34—C37—C44—O45	179.6	179.5	

[a] This work.
[b] From Refs [33,34].

interest as possible drug candidate, as suggested by Veber and Lipinski [38,39]. Hence, the atomic Merz-Kollman (MK) and natural population atomic (NPA) charges and the molecular electrostatic potential (MEP) in this acetogenin were studied in gas phase and in methanol solution only for the atoms belonging to the three R1, R2 and R3 rings and to the OH groups. Fig. 2 shows the atoms labelling involved in the three considered moietis of squamocin which are indicated in the figure by circles while in Table 3 are presented the calculated MK and NPA charges and MEP values by using the hybrid B3LYP/6-31G* method. The variations of both MK and NPA charges on the three rings are easily observed in Fig. 3. Analyzing first the MK charges on the O and C atoms of ring R1 from Fig. 3a we observed that practically present the same values in both media, with exception of charge on C5 which has positive sign and a null value in gas phase. The NPA charges present different values and in general higher than the MK ones and show the same behaviours in the two media. Lower NPA values are observed on the O1, O2, C3 and C5 atoms while these charges on the C4 and C6 atoms increase in both media.

When the MK charges are evaluated on the atoms of the two R2 and R3 rings from Fig. 3b we observed different values in both media, in particular, the charge on C44 increases in methanol solution while on O48 decreases in this medium. The NPA charges on all considered atoms evidence the same behaviours in both media but sligthly different from the MK charges. These studies with the two types of charges show that the O atoms of R2 and R3 ring in both media present higher values than the observed on O atoms of lactone R1 ring.

When the molecular electrostatic potential (MEP) values for squamocin in the different media are analyzed from Table 3 the values practically remain constant and there are no significant changes in them. The only differences observed are in the values for the different atoms which, as expected, present the following trend: O > C > H. On the other hand, when the mapped MEP surfaces for squamocin in both media are graphed from the *GaussView* program [22] it is possible to predict the main nucleophilic and electrophilic sites where the reactions with potential electrophiles or nucleophiles take place. Thus, for squamocin in methanol solution these mapped MEP surfaces by using the B3LYP/6-31G* level of theory can be seen in Fig. S2. The graphic shows different positions for squamocin in methanol solution in order to see clearly the red and blue colorations. Thus, the strong red colours can be seen on the O atoms belonging to the three rings, including the lactone one, and on the O89 atom (see Fig. 2) that belong to O89—H90 bond (upper Fig. S2). Then, these red colorations evidence that the nucleophilic regions are located on the O atoms of three rings and on the O atom of OH bond belonging to side chain. These resulted is in agreement with the higher MK and NPA charges values evidenced on the O atoms, as detailed in Table 3. On the other side, blue colours are shown on the H atoms of OH bonds revealing that these sites are clearly electrophilic regions. Note that the large aliphatic side chains are inert regions which present green colours. These studies show that in both media the nucleophilic regions are more extense than the electrophilic one and, probably for these reasons, squamocin reveals a high nucleophilic index and a higher reactivity in methanol solution, as compared with the corresponding values in gas phase, as we will see later.

4.3. NBO and AIM studies

Previous studies on squamocin in both media have shown different nucleophilic and electrophilic sites distributted in the large aliphatic chain evidencing that in this acetogenin the acceptors and donors groups present in its structure have a role fundamental in the antimicrobial and cytotoxic activities reported [13,16—21]. Hence, natural bond orbital (NBO) and atoms in molecules (AIM) calculations were performed in order to investigate if the different positions of the acceptor and donors groups (O and OH groups) in squamocin have some influence on its stability in both media [28—30]. Hence, first the donor-acceptor energy interactions were calculated for squamocin in both media by using the Second Order Perturbation Theory Analysis of Fock Matrix in NBO Basis with the hybrid B3LYP/6-31G* method and by using NBO calculations [28]. The results are presented in Table 4 and show four different $\Delta E_{\pi\rightarrow\pi^*}$, $\Delta E_{n\rightarrow\pi^*}$, $\Delta E_{n\rightarrow\sigma^*}$ and $\Delta E_{\pi^*\rightarrow\pi^*}$ interactions in the two media as a consequence of C═O, C═C and C—O groups present

Table 3
Calculated MK and NPA charges (in a.u.) and molecular electrostatic potential values (in a.u.) for squamocin acetogenin in gas phase and methanol solution by using the hybrid B3LYP/6-31G* method.

B3LYP/6-31G* method						
Atoms	Gas phase			Methanol solution		
	MK	NPA	MEP	MK	NPA	MEP
Lactone R1 rings						
1 O	−0.345	−0.518	−22.263	−0.350	−0.514	−22.261
2 O	−0.445	−0.534	−22.332	−0.458	−0.537	−22.334
3C	0.462	0.399	−14.658	0.473	0.394	−14.657
4C	−0.467	−0.322	−14.726	−0.461	−0.319	−14.724
5C	0.022	−0.089	−14.719	−0.019	−0.085	−14.718
6C	0.544	0.724	−14.629	0.564	0.719	−14.629
R2 and R3 rings						
33C	0.522	0.069	−14.692	0.586	0.069	−14.693
34 O	−0.569	−0.619	−22.311	−0.584	−0.617	−22.313
35C	−0.478	−0.490	−14.734	−0.502	−0.488	−14.735
44C	0.248	0.084	−14.690	0.355	0.081	−14.691
45 O	−0.586	−0.593	−22.320	−0.598	−0.593	−22.323
46C	−0.175	−0.478	−14.735	−0.183	−0.477	−14.735
47H	0.032	0.213	−1.128	−0.006	0.212	−1.128
48C	0.385	0.072	−14.687	0.338	0.071	−14.689
49C	−0.107	−0.487	−14.730	−0.079	−0.487	−14.731
C−O−H groups						
55C	0.251	0.090	−14.691	0.283	0.088	−14.691
56H	0.078	0.230	−1.126	0.077	0.231	−1.124
57 O	−0.602	−0.743	−22.322	−0.610	−0.742	−22.323
58H	0.394	0.462	−1.002	0.395	0.460	−1.003
65C	−0.363	−0.477	−14.744	−0.283	−0.477	−14.742
66H	0.086	0.231	−1.125	0.067	0.230	−1.122
67H	0.084	0.216	−1.125	0.067	0.216	−1.123
68C	0.275	0.107	−14.693	0.245	0.106	−14.691
69H	0.069	0.225	−1.130	0.076	0.225	−1.128
70C	−0.274	−0.477	−14.745	−0.306	−0.476	−14.744
71H	0.063	0.232	−1.126	0.068	0.231	−1.128
87H	0.067	0.224	−1.134	0.064	0.224	−1.133
88H	0.067	0.224	−1.134	0.065	0.224	−1.133
89 O	−0.622	−0.754	−22.321	−0.626	−0.755	−22.321
90H	0.408	0.461	−1.002	0.410	0.460	−1.002
91H	−0.557	−0.766	−22.334	−0.542	−0.767	−22.336

in the lactone ring (R1). Hence, the total energy favours to squamocin in methanol solution with a value of 799.27 kJ/mol while in gas phase the value decrease to 745.71 kJ/mol. These values are different from those observed in motrilin acetogenin where the total energy value of 786.63 kJ/mol in methanol solution and of 745.71 kJ/mol in gas phase [13]. In both acetogenins, the high stabilities observed in methanol solution probably can be justified by a higher solute-solvent association due to the H bonds formation in methanol solution and to the low permittivity of solvent ($\varepsilon = 32.613$).

The Bader's theory of atoms in molecules (AIM) through calculations of topological properties allows to analyze different intra-or inter-molecular interactions [29]. Accordingly, the electron density distribution, $\rho(r)$ and the Laplacian values, $\nabla^2\rho(r)$, the eigenvalues ($\lambda1$, $\lambda2$, $\lambda3$) of the Hessian matrix and the $\lambda1/\lambda3$ ratio in the bond critical points (BCPs) and in the ring critical points (RCPs) were calculated with the version 2000 of AIM program [30]. Here, the results for squamocin in both media are given in Table 5. In both media, only a H bond was observed whose properties are $\lambda1/\lambda3 < 1$ and $\nabla^2\rho(r) > 0$. Molecular models of squamocin in methanol solution are presented in two graphics in Fig. S3 and these correspond to two parts of its structure because it present a large aliphatic chain. In both cases, the new H bond created correspond to O91−H92···O34 interaction formed between the groups corresponding to ring R2. It interaction form a new RCP named RCPN1 while the other R1, R2 and R3 rings only present the RCP1, RCP2 and RCP3. Here, RCP2 and RCP3 can be seen in the upper graphic while the RCP1 in the inferior graphic of Fig. S3. The properties presented in Table 5 show that the distance between the involved O34 and H92 atoms in the new H bond formed is higher in methanol solution (2.1128 Å) than the value in gas phase (2.0640 Å), indicating that this interaction is stronger in gas phase than in solution. Hence, the densities values justify these latter observations. Another important observation is the decreasing in the density value of RCP1 in solution which belong to lactone ring, as compared with the value in gas phase. This fact was also observed in the motrilin acetogenin [13] and, in that case, the decreasing was atributted to the solvation of O atoms with solvent molecules increasing the electron density of R1 ring. Then, the intensity of band associated to C═O stretching mode in methanol solution increase, as was also observed in squamocin.

4.4. Frontier orbitals and global descriptors

The mapped MEP surfaces have evidenced that in the two media the nucleophilic regions (seven acceptors atoms) are more extense than the electrophilic one (three donors OH groups) and while the NBO study support the high stability of squamocin in methanol solution. On the other hand, the acceptors (O) and donors (O−H) groups present in the squamocin structure probably support the antimicrobial and cytotoxic properties revealed for this γ-lactone [13,16–21]. For the above reasons, frontier orbitals [16,17] and some global descriptors should be investigated for squamocin in both media [18–21]. First, the gap values for squamocin were calculated in both media with the values of frontier orbitals by using the B3LYP/6-31G* method and, then, with these gap values the

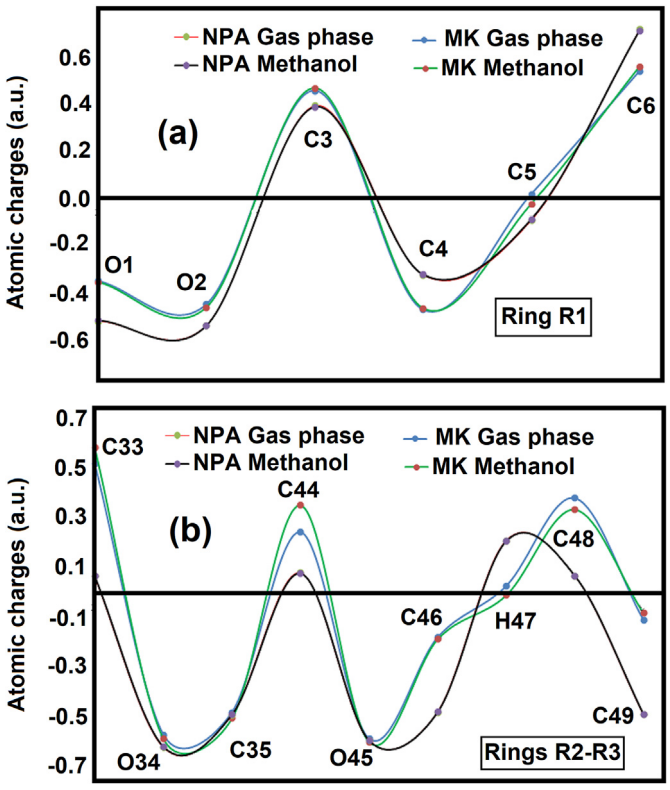

Fig. 3. Behaviours of MK and NPA charges on the three rings of the most stable conformer of squamocin in gas phase and methanol solution by using B3LYP/6-31G* method.

chemical potential (μ), electronegativity (χ), global hardness (η), global softness (S), global electrophilicity index (ω) and nucleophilicity indexes (E) descriptors were computed by using known equations [18–21]. Thus, in Table 6 are summarized the calculated HOMO and LUMO, energy band gaps and those mentioned descriptors for squamocin in gas phase and methanol solution by using the hybrid B3LYP/6-31G* method. The equations used to calculate the descriptors are presented in the same Table together with frontier orbitals, gap values and descriptors reported for motrilin, 6-nitro-1,3-benzothiazole-2(3H)-thione and niclosamide species with different biological activities [13,31,32]. Motrilin is an acetogenin as squamocin while the benzothiazol-thione derivative has potential antimicrobial activity and, niclosamide was suggested as potential antiviral to treatment of COVID-19 [13,31,32,40]. When the gap values for squamocin are compared in both media it is observed that the value observed in methanol solution (3.7195 eV) is slightly lower than the observed in gas phase (3.8069 eV). Hence, squamocin is most reactive in methanol solution, as also was predicted for motrilin. This latter acetogenin is most reactive in both media than squamocin because their gap values have lower values. On the other hand, ascorbic acid is less reactive than the two acetogenins (5.5071 eV) while the benzothiazole derivative is the most reactive than all compared compounds, with a gap value of 3.6525 eV. Here, a very important resulted is observed in the two global electrophilicity index (ω) and nucleophilicity (E) indexes, that is, when the gap values are between 3.6 and 3.8 eV the electrophilicity index (ω) are 5.7/5.9 eV while the nucleophilicity indexes (E) are −8.4/-8.9 eV. On the contrary, the ascorbic acid ω has a value of 2.1673 eV while the value of E is-9.5128 eV. Another important resulted obtained here is that the large aliphatic chains in both acetogenins produce decreasing in the gap values, as compared with ascorbic acid, indicating this way that the large

Table 4
Main donor-acceptor energy interactions (in kJ/mol) for squamocin acetogenin in gas phase and methanol solution by using the hybrid B3LYP/6-31G* method.

B3LYP/6-31G*		
Delocalization	Gas phase	Methanol solution
$\pi C5\text{-}C6 \rightarrow \pi^* C3\text{–}C4$	66.42	77.99
$\Delta ET_{\pi \rightarrow \pi^*}$	**66.42**	**77.99**
$LPO1 \rightarrow \pi^* C3\text{–}C4$	52.42	49.11
$LPO1 \rightarrow \pi^* C5\text{–}C6$	60.86	64.91
$LPO2 \rightarrow \pi^* C5\text{–}C6$	210.13	200.47
$\Delta ET_{LP \rightarrow \pi^*}$	**323.41**	**314.49**
$LPO2 \rightarrow \sigma^* O1\text{–}C6$	85.77	80.80
$\Delta ET_{LP \rightarrow \sigma^*}$	**85.77**	**80.80**
$\pi^* C5\text{–}C6 \rightarrow \pi^* C3\text{–}C4$	270.11	325.99
$\Delta ET_{\pi^* \rightarrow \pi^*}$	**270.11**	**325.99**
ΔE_{Total}	**745.71**	**799.27**

Table 5
Analyses of the topological properties for squamocin acetogenin in gas phase and methanol solution by using the hybrid B3LYP/6-31G* method.

B3LYP/6-31G* Method										
Gas phase						Methanol solution				
Parameter[#]	RCP1	RCP2	RCP3	RCPN1	O34···H92	RCP1	RCP2	RCP3	RCPN1	O34···H92
$\rho(r)$	0.0392	0.0388	0.0463	0.0207	0.0220	0.0389	0.0386	0.0467	0.0200	0.0209
$\nabla^2\rho(r)$	0.2785	0.2745	0.3571	0.1133	0.0851	0.2756	0.2728	0.3588	0.1056	0.0808
$\lambda 1$	−0.0420	−0.0415	−0.0492	−0.0193	−0.0254	−0.0415	−0.0413	−0.0497	−0.0186	−0.0235
$\lambda 2$	0.1573	0.1540	0.1986	0.0245	−0.0177	0.1552	0.1529	0.2019	0.0201	−0.0149
$\lambda 3$	0.1632	0.1619	0.2076	0.1080	0.1282	0.1621	0.1615	0.2069	0.1042	0.1195
$\lvert\lambda 1\rvert/\lambda 3$	0.2573	0.2563	0.2370	0.1787	0.1973	0.2560	0.2557	0.2402	0.1785	0.1966
Distances (Å)					2.0640					2.1128

Table 6
Calculated HOMO and LUMO, energy band gap, chemical potential (μ), electronegativity (χ), global hardness (η), global softness (S), global electrophilicity index (ω) and global nucleophilicity index (E) for squamocin acetogenin in gas phase and methanol solution by using the hybrid B3LYP/6-31G* method.

Frontier orbitals (eV)	B3LYP/6-31G* method			
	Squamocin[a]		Ascorbic acid[b]	
	Gas phase	Methanol solution		
HOMO	−6.5716	−6.5179	−6.2083	
LUMO	−2.7647	−2.7984	−0.7012	
|GAP|	3.8069	3.7195	5.5071	
Descriptors (eV)				
χ	−1.9035	−1.8598	−2.7536	
μ	−4.6682	−4.6582	−3.4548	
η	1.9035	1.8598	2.7536	
S	0.2627	0.2689	0.1816	
ω	5.7242	5.8337	2.1673	
E	−8.8856	−8.663	−9.5128	
B3LYP/6-31G* method				
Frontier orbitals (eV)	Motrilin[b]		Thione[c]	Niclosamide[d]
	Gas phase	Methanol solution		
HOMO	−6.5335	−6.5004	−6.4443	−6.5688
LUMO	−2.7620	−2.8012	−2.7918	−2.8436
|GAP|	3.7715	3.6992	3.6525	3.7252
Descriptors (eV)				
χ	−1.8858	−1.8496	−1.8263	−1.8626
μ	−4.6478	−4.6508	−4.61805	−4.7062
η	1.8858	1.8496	1.8263	1.8626
S	0.2651	0.2703	0.2738	0.2684
ω	5.7276	5.8472	5.8388	5.9455
E	−8.7645	−8.6021	−8.4337	−8.7658

χ = - [E(LUMO) - E(HOMO)]/2; μ = [E(LUMO) + E(HOMO)]/2; η = [E(LUMO) − E(HOMO)]/2; S = ½η; $\omega = \mu^2/2\ \eta$; $E = \mu$ *η
[a] This work.
[b] From Ref [13].
[c] From Ref [31].
[d] From Niclosamide in ethanol Ref [32].

aliphatic chains increase the reactivities in the two acetogenins. This latter result was also observed when the length of their side chain increases from cidofovir up to brincidofovir [41].

4.5. Vibrational analyses

Squamocin is an acetogenin with 109 atoms and, for this reason, the assignments of main vibrational normal modes of squamocin were performed with the aid of *GaussView* program [22] and by comparisons with assignments reported for species containing similar groups [13,18−22]. Hence, the harmonic force fields of aquamocin in both media were not calculated with the scaled quantum mechanical force field (SQMFF) methodology [42] and due to the 109 atoms present in its structure 321 vibration normal modesare expected for squamocin, where only 129 vibration modes were assigned. The experimental FT-IR and FT-Raman spectra of squamocin in the solid phase are presented in Figs. 4 and 5 compared with the corresponding predicted in the gas phase and methanol solution by using the B3LYP/6-31G* method. To a better correlation between experimental and theoretical Raman spectra, those two Raman spectra predicted for squamocin in gas phase and aqueous solution in activities were transformed to intensities [43,44]. The assignments of the main bands observed in the vibrational spectra of squamocin are presented in Table 7. Here, these assignments proposed for squamocin were compared with assignments reported in the literature for similar groups [13,18−21,31,32,34,35,41]. In this work, taking into account the annharmonicity predicted in the 4000-2500 cm^{-1} region for the O−H, C−H, CH_2 and CH_3 stretching modes their calculated frequencies were scaled by using the scale factor 0.919, as suggested in the literature for that basis set used [42]. Fig. 4 shows that the predicted FT-IR spectrum of squamocin in gas phase is different from that predicted in methanol solution in the regions between 4000 and 2500 cm^{-1} and between 2000 and 10 cm^{-1}. Thus, in those two different regions are observed that intensities and positions of some bands associated to strectching modes of C═O and OH groups change in solution due to solvent effect, as can be seen in Fig. S4. Thus, in the higher wavenumber region Fig. S4 shows that the band related to OH stretching mode of squamocin is shifted in methanol solution while its intensity slighlty increase while the band associated to C═O stretching mode is predicted shift toward lower wavenumber and with higher intensity in methanol solution, as compared with the predicted spectrum in gas phase. Besides, in the 500 and 300 cm^{-1} region some bands increase its intensities as consequence of solvation with solvent molecules, as also can be seen in Fig. S4. The most important assignments are discussed at continuation by regions.

4.5.1. Band assignments

4.5.1.1.4000−2000 cm^{-1} region. In this region, the stretching modes of O−H, C−H, CH_3 and CH_2 groups are expected. Here, the calculated IR bands for these vibration modes have been scaled by using the scale factor 0.919, as suggested in the literature for the 6-31G* basis set [42]. These modes in ascorbic acid were assigned between 3523 and 3030 cm^{-1} [21]. Squamocin present three OH groups, as motrilin [13] but differ of it in the position of the OH group linked to the sides chains. In this acetogenin, these modes are predicted at 3415, 3410 and 3398 cm^{-1}, as in similar groups [13,18,20,21,31,32,34,35]. Hence, the IR bands at 3427 and 3388 cm^{-1} are assigned to three O−H stretching modes. The aromatic C−H stretching mode corresponding to lactone ring is predicted by calculations at 3250 cm^{-1}, hence, this stretching mode is located at higher wavenumber than the other aliphatic ones. But with the scaling process it mode is shifted at 2986 cm^{-1} and, hence, it can be assigned to the Raman band at 3079 cm-1 B3LYP/6-31G* calculations predict the other aliphatic C−H stretching modes at

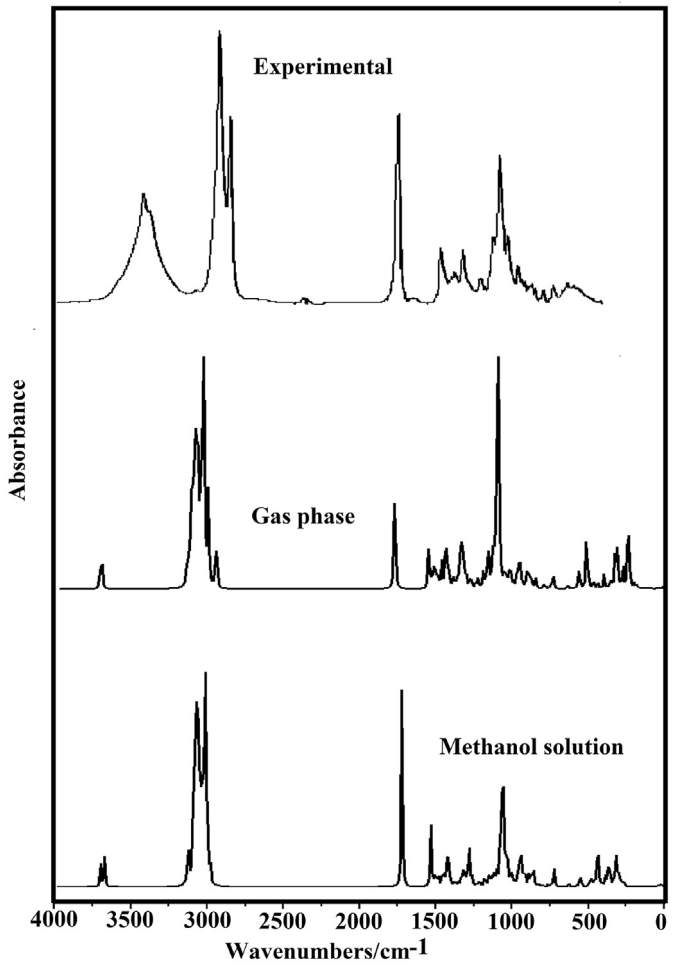

Fig. 4. Experimental infrared spectra of squamocin in the solid state compared with the corresponding predicted in gas phase and methanol solution by using hybrid B3LYP/6-31G* method.

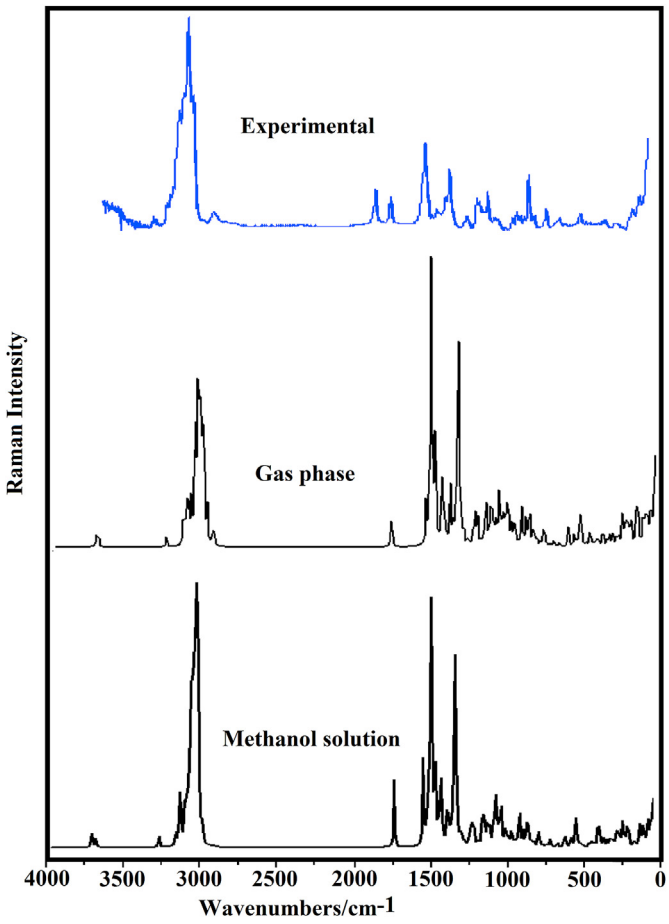

Fig. 5. Experimental Raman spectra of squamocin in the solid state compared with the corresponding predicted in gas phase and methanol solution by using hybrid B3LYP/6-31G* method.

2998 cm^{-1} and, with the scaling these modes appear at 2775 cm^{-1}. For this reason, the Raman band at 2725 cm^{-1} can be assigned to these vibration modes. In squamocin there are two CH_3 groups where one of them belong to the lactone ring and the other one is located at end of the long side chain, as observed in Fig. 2. This ACG has twenty-four CH2 groups of which twenty belong to the side chain and the remaining four to the R2 and R3 rings, where, the antisymetric and symmetric modes of those groups are predicted by calculations coupled among them. For these reasons, and due to elevated number of bands only some of these are assigned to those modes, as observed in Table 7. Those antisymmetric CH_3 and CH_2 stretching modes are predicted at higher wavenumbers than the corresponding symmetric ones and, hence, the IR and Raman bands between 3008 and 2844 cm^{-1} are assigned to those stretching modes. The corresponding symmetric stretching modes are assigned to the IR and Raman bands between 2932 and 2844 cm^{-1}. Note that the intense Raman bands are assigned to symmetric stretching modes, as expected.

4.5.1.2.2000–1000 cm^{-1} region. The characteristics vibrations expected in this region are the C═O, C═C, C–O and C–C stretching modes, OH and CH in-plane deformation modes and, also the deformation, wagging and rocking modes of CH_3 and CH_2 groups. The C═O and C═C stretching modes of lactone ring are predicted respectively at 1773 and 1550 cm^{-1} and are easily assigned to the IR and Raman bands located respectively at 1744 and 1649 cm^{-1}. In ascorbic acid those two stretching modes were assigned at 1753 and 1672 cm^{-1} [21]. On the other hand, the antisymmetric and symmetric deformation modes of CH_3 and CH_2 groups are predicted by calculations between 1543 and 1441 cm^{-1}, hence, according to the calculations they are assigned as in similar species containing these groups [13,18,34,35,41]. The CH in-plane deformation modes (ρC-H) are assigned to the IR and Raman bands between 1499 and 1300 cm^{-1}, as predicted by calculations while for the OH groups these modes are assigned between 1281 and 1136 cm^{-1}. The bands between 1409 and 1265 cm^{-1} can be assigned to CH_2 wagging modes while the located between 1342 and 1192 cm^{-1} are assigned to rocking of CH_2 groups. The CH_3 rocking modes of groups are predicted and assigned to the bands between 1057 and 904 cm^{-1}. The group of IR and Raman bands between 1171 and 792 cm^{-1} can be assigned to C–C and C–O stretching modes because the B3LYP/6-31G* calculations predict clearly these modes in that region [13,34,35,41].

4.5.1.3.1000–20 cm^{-1} region. The out-of-plane OH and C–H deformation modes, of twisting modes of CH_2 and CH_3 groups, skeletal modes such as, in-plane βC = O and βC-C deformation or out-of-plane γC = O, γC-C deformation modes and of deformation rings (βR1, βR_2) and torsion rings (τR1, $\tau R2_)$ modes of five members R1, R2 and R3 rings are expected in this region. Those vibration modes are strongly coupled among them due to great quantity of observed bands in the same positions. The out-of-plane OH

Table 7
Observed and calculated wavenumbers (cm^{-1}) and assignments for squamocin acetogenin in gas phase by using the hybrid B3LYP/6-31G* method.

Squamocin[a]			
Experimental		B3LYP/6-31G*	
IR	Ra	SQM[b]	Assigment[a]
3427 m		3415	νO-H
3427 m		3410	νO-H
3388 m		3398	νO-H
3083sh	3079w	2986	νC-H
	3008w	2891	$\nu_a CH_3$
	2983w	2884	$\nu_a CH_2$
2971sh	2970w	2876	$\nu_a CH_2$
2953sh	2950w	2867	$\nu_a CH_2$
		2864	$\nu_a CH_2$
		2860	$\nu_a CH_3$
	2932s	2854	$\nu_a CH_3$
2923vs		2841	$\nu_a CH_3$
2901sh	2904s	2823	$\nu_s CH_2$
	2877vs	2813	$\nu_s CH_2$
2852s	2844s	2796	$\nu_s CH_3$
	2844s	2793	$\nu_s CH_2$
	2725w	2755	νC-H
1744s	1740w	1773	$\nu C = O$
1649w	1649w	1550	C=C
1649w	1649w	1543	$\delta_a CH_3$
1649w	1649w	1530	$\delta_a CH_3$
1508w		1503	δCH_2
1489w		1499	ρC-H
1473sh	1476sh	1495	$\delta_a CH_3$
1465 m		1485	$\delta_a CH_3$
1459 m	1455sh	1463	ρC-H
1450w		1449	ρC-H
1439w	1441 m	1441	$\delta_s CH_3$
1418w	1421w	1420	ρC-H
1397w	1397w	1409	$wagCH_2$
1397w		1394	$wagCH_2$
1389w		1388	ρC-H
1374w	1368w	1374	ρC-H
1374w		1366	ρC-H
1363w		1361	$wagCH_2$
1355w	1352w	1354	$wagCH_2$
1355w		1342	ρCH_2
1337sh		1337	ρCH_2
1319 m		1321	ρCH_2
1319 m	1319w	1319	ρC-H
1319 m		1311	$wagCH_2$
1304sh	1301sh	1305	ρCH_2
		1300	ρC-H
1287w	1293w	1282	ρCH_2
		1281	δO-H
1273w	1270w	1270	δO-H
1253w	1252vw	1265	$wagCH_2$
1230w	1227vw	1227	ρCH_2
1205w	1208vw	1212	ρCH_2
	1201vw	1192	ρCH_2
	1188w	1181	βC-H
1172w	1172w	1171	νC-C
1146w	1144w	1152	νC-C
1146w	1144w	1136	δO-H
1128sh	1130w	1126	νC-O
1121 m	1112w	1124	νC-O
1089sh	1088vw	1114	νC-O
1076s	1075vw	1095	νC-O
1071sh	1061 m	1072	νC-C
		1059	νC-C
1053 m		1057	ρCH_3
	1046w	1046	νC-C
1027 m	1024w	1027	νC-C
	1013w	1019	ρCH_3
1000w	996w	997	νC-C
980w	979w	979	νC-C
960w	960w	967	νC-C
953w	945w	955	νC-C
928w		932	νC-C
928w	921sh	927	νC-C
911w	908w	911	νC-C

(*continued on next page*)

Table 7 (*continued*)

Squamocin[a]			
Experimental		B3LYP/6-31G*	
911w	908w	904	ρCH_3
889w	888w	892	νC-O
878w	877w	887	τwCH_2
861w	860w	860	τwCH_2
840w	839w	850	γC-H
840w	839w	846	ρCH_3
809w	812 m	811	τwCH_2
791w	790sh	792	νC-O
779sh	776w	777	τwCH_2
758w	756vw	756	τwCH_2
744w		746	τwCH_2
722w	704w	728	$\gamma C=O$
698sh	658w	694	βR_1 (A1)
660w	645w	644	βR_1 (A3)
630w	633w	636	βR_1 (A2)
620sh	625w	610	βR_2 (A2)
607vw		603	βR_2 (A3)
590w	590w	592	τwCH_2
568sh		564	$\beta C=O$
561w	557vw	557	δCCC
541sh	540vw	537	δCCC
	522vw	515	τO-H
509sh	509sh	506	τO-H
	499w	497	δCCC
488w	489sh	484	δCCC
476sh		471	δCCC
465w	462w	463	δCCC
448w	443w	445	δCCC
437sh		440	δCCC
424w		438	δCCC
414w	410w	414	δCCO
	399w	399	δCCO
	389vw	392	δCCO
		382	δCCO
		366	δCCC
	364vw	359	δCCC
	345vw	344	δCCC
	322	326	τO-H
		312	τO-H
		304	βC-C
	288vw	292	δCCC
		277	βC-C
	262sh	275	δCCC
	248vw	249	τwCH_3
	248vw	242	τO-H
	248vw	227	τO-H
	202sh	203	δCCO
	191sh	196	τR_1 (A3)
	183w	186	τR_1 (A1)
	168sh	169	τwC-C
	140w	143	τwCH_3
	119sh	124	τwC-C
	104sh	116	τwCH_3
	86sh	88	τwC-C
	68sh	68	τwC-C
		42	τwC-C
		38	τwC-C
		24	τwC-C

Abbreviationsν, stretching; wag, wagging; τ, torsion; ρ, rocking; τw, twisting; δ, deformation; a, antisymmetric; s, symmetric.

[a] This work.

[b] From SQMFF B3LYP/6-31G* method only for the bands observed in the 4000-2000 cm-1 region. From 2000 to 400 cm-1 by the B3LYP/6-31G* method.

deformation modes or torsion modes are predicted and assigned at 515, 506, 326, 312 and 248 cm^{-1} while the out-of-plane deformation mode for aromatic C—H group of lactone ring (γC-H) is assigned to the weak IR and Raman bands respectively at 840 and 839 cm^{-1}. The calculations predict the twisting modes of two CH_3 groups with weak intensities at 249, 143 and 116 cm^{-1}, hence, these modes can be associated to the Raman bands and the shoulder in the same spectrum at 248, 140 and 104 cm^{-1}. The CH_2 twisting modes are normally assigned between 1041 and 558 cm^{-1} [13,18,34,35,41], thus, in this ACG these modes are assigned to the bands between 878 and 590 cm^{-1}. The assignments of other skeletal modes are performed according to the calculations and by comparisons with species with similar groups [13,18–21,32,34,35,41], can be seen in Table 7.

5. Ultraviolet–visible spectrum

The experimental UV—visible spectrum of squamocin in

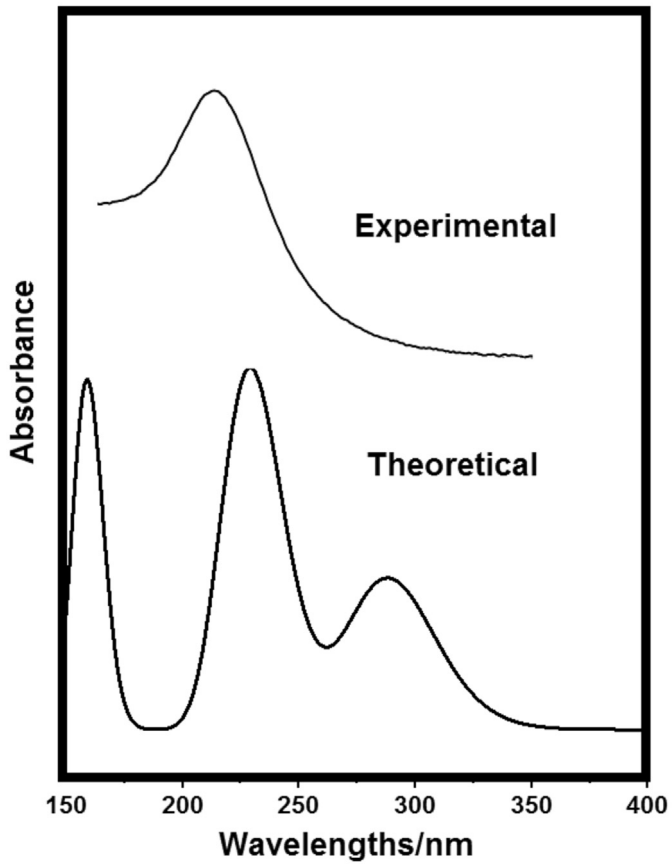

Fig. 6. Experimental Utraviolet-visible spectra of squamocin in methanol solution compared with the corresponding predicted in the same medium by using hybrid B3LYP/6-31G* method.

methanol solution is shown in Fig. 6 compared with the corresponding predicted in the same medium by using the B3LYP/6-31G* method. The electronic spectrum of this γ-lactone was predicted with TD-DFT calculations incorporated in the Gaussian09 program [23]. The experimental spectrum shows a very strong band at 213 nm while in the predicted spectrum are observed two intense bands in c. a. 160 and 230 nm and, other weak in c. a. 288 nm. The experimental spectrum was recorded from 200 up to 400 nm and, for this reason, the band predicted between 150 and 200 nm was not experimentally observed. In the experimental UV−Vis spectrum of motrilin ACG in methanol solution the intense band is observed at 220 nm [13]. The NBO calculations predict $\pi \rightarrow \pi^*$ and $n \rightarrow \pi^*$ transitions and, hence, those predicted bands can be assigned to those two transitions due to C═C and C═O bonds of γ-lactone, as assigned in similar compounds [13,18,20,45,46].

6. Conclusions

Squamocin acetogenin has been isolated and characterized by using the FT-IR and FT-Raman spectra in the solid phase and the UV−Visible spectrum in methanol solution. Its theoretical molecular structures were determined in gas phase and methanol solution by using the hybrid B3LYP/6-31G* method. The calculations in solution were carried out with the IEFPCM and solvation models. The structural, electronic and topological properties for the most stable structure in both media were predicted at the same level of theory. The main bands observed in the vibrational spectra were assigned combining the IR and Raman spectra with hybrid functional B3LYP/6-31G* calculations. A corrected solvation energy value of −147.54 kJ/mol was predicted for squamocin in methanol while the atomic NPA charges evidence higher values on O atoms of R2 and R3 rings, as compared with the corresponding to lactone ring. Mapped MEP surfaces suggest that nucleophilic regions are located on the O atoms of three rings and of OH bonds belonging to side chain, in agreement with the higher charges values evidenced on these O atoms while electrophilic regions are predicted on the H atoms of OH groups. AIM studies have revealed high stabilities of squamocin in both media while the NBO calculations show higher stability only in methanol solution. The expansion of volume and the higher dipole moment in methanol suggest a clear solvation of squamocin by solvent molecules. The gap values have evidenced that squamocin is most reactive in methanol while that its large aliphatic chain produces an increases in the reactivity of this γ-lactone, as compared with ascorbic acid lactone. Reasonable concordances among the predicted IR, Raman and UV−visible spectra with the corresponding experimental ones were found.

Declaration of competing interest

The authors declare that they have no known competing financial interests or personal relationships that could have appeared to influence the work reported in this paper.

CRediT authorship contribution statement

José Ruiz Hidalgo: Conceptualization, Data curation, Supervision. **Adriana Neske:** Methodology, Data curation. **Maximiliano A. Iramain:** Conceptualization, Data curation. **Patricia E. Alvarez:** Conceptualization, Project administration. **Patricio Leyton Bongiorno:** Methodology, Resources. **Silvia Antonia Brandán:** Validation, Visualization, Writing - original draft, Writing - review & editing.

Acknowledgements

This work was supported with grants from CIUNT Project N° 26/D608 (Consejo de Investigaciones, Universidad Nacional de Tucumán).

Appendix A. Supplementary data

Supplementary data to this article can be found online at https://doi.org/10.1016/j.molstruc.2020.128610.

References

[1] D. Cortes, S.H. Myint, Reynald Hocquemiller, Molvizarin, Motrilin, Two novel cytotoxic bis-tetrahydrofuranic y-lactone acetogenins from *Annona cherimolia*, Tetrahedron 47 (38) (1991) 8195−8202.
[2] I. Barrachina, A. Neske, S. Granell, A. Bermejo, N. Chahboune, N. El Aouad, O. Alvarez, A. Bardon, M.C. Zafra-Polo, Tucumanin, a B-Hydroxy G-Lactone Bistetrahydrofuranic Acetogenin from Annona Cherimolia, Potent Inhibitor of Mitochondrial Complex I (2004).
[3] H. Yang, N. Zhang, X. Li, J. Chen, B. Cai, Structure−activity relationships of diverse annonaceous acetogenins against human tumor cells, Bioorg. Med. Chem. Lett 19 (2009) 2199−2202.
[4] J.A. Bombasaro, L. Di Toto Blessing, S. Diaz, A. Neske, F.D. Suvire, R.D. Enriz, A.M. Rodríguez, Theoretical and experimental study of the interactions of annonaceous acetogenins with artificial lipid bilayers, J. Mol. Struct. 1003 (2011) 87−91.
[5] Y. Chen, J-w Chen, X. Li, Monotetrahydrofuran annonaceous acetogenins from the seeds of Annona squamosa, Phytochemistry Letters 5 (2012) 33−36.
[6] J.C. Ramos, Síntesis quimioenzimática de anillos THF presentes en acetogeninas, Doctoral Thesis, Universidad de la República de Uruguay, 2014.
[7] J. Hong, Y. Li, Y. Xiao, Y. Li, Y. Guo, H. Kuang, X. Wang, Annonaceous acetogenins (ACGs) nanosuspensions based on aself-assembly stabilizer and the significantly improved anti-tumor efficacy, Colloids Surf. B Biointerfaces 145

(2016) 319–327.
[8] Y.-J. Miao, Y.-Y. Shi, X.-F. Xu, Y. Chen, J.-W. Chen, X. Li, Three cytotoxic Annonaceous acetogenins from the seeds of *Annona squamosa*, Phytochemistry Letters 16 (2016) 92–96.
[9] J. Ruiz Hidalgo, E.A. Parellada, L. Di Toto Blessing, A. Bardón, K. Lalit Ameta, N. Vera, A. Neske, Natural and derivatized acetogenins promising for the control of *Spodoptera frugiperda* smith, J. Agric. Chem. Environ. 5 (2016) 200–210.
[10] A. Attiq, J. Jalil, K. Husain, Annonaceae: breaking the wall of inflammation, Front. Pharmacol. 8 (2017). Article 752.
[11] J. Hong, Z. Sun, Y. Li, Y. Guo, Y. Liao, M. Liu, X. Wang, Folate-modified Annonaceous acetogenins nanosuspensions and their improved antitumor efficacy, Int. J. Nanomed. 12 (2017) 5053–5067.
[12] P.E. Alvarez, M.V. Fiori-Bimbi, A. Neske, S.A. Brandán, C.A. Gervasi, Rollinia occidentalis, extract as green corrosion inhibitor for carbon steel in HCl solution, J. Ind. Eng. Chem. 58 (2018) 92–99.
[13] J. Ruiz Hidalgo, A. Neske, M.A. Iramain, P.E. Alvarez, P. Leyton Bongiorno, S.A. Brandán, FT-IR, FT-Raman and UV-visible spectra of motrilin acetogenin isolated from *Annona cherimolia*, J. Mol. Struct. 1196 (2019) 508–517.
[14] A.D. Becke, Density-functional exchange-energy approximation with correct asymptotic behavior, Phys. Rev. A38 (1988) 3098–3100.
[15] C. Lee, W. Yang, R.G. Parr, Development of the Colle-Salvetti correlation-energy formula into a functional of the electron density, Phys. Rev. B 37 (1988) 785–789.
[16] R.G. Parr, R.G. Pearson, Absolute hardness: companion parameter to absolute electronegativity, J. Am. Chem. Soc. 105 (1983) 7512–7516.
[17] J.-L. Brédas, Mind the gap!, Materials Horizons 1 (2014) 17–19.
[18] M. Minteguiaga, E. Dellacassa, M.A. Iramain, C.A.N. Catalán, S.A. Brandán, Synthesis, Spectroscopic characterization and structural study of carquejiphenol, a 2-Isopropenyl-3-methylphenol derivative with potential medicinal uses, J. Mol. Struct. 1165 (2018) 332–343.
[19] S. Gatfaoui, N. Issaoui, S.A. Brandán, T. Roisnel, H. Marouani, Synthesis and characterization of p-xylylenediaminiumbis(nitrate). Effects of the coordination modes of nitrate groups on their structural and vibrational properties, J. Mol. Struct. 1151 (2018) 152–168.
[20] R.A. Rudyk, M.A. Checa, C.A.N. Catalán, S.A. Brandán, Structural, FT-IR, FT-Raman and ECD spectroscopic studies of free base, cationic and hydrobromide species of scopolamine alkaloid, J. Mol. Struct. 1180 (2019) 603–617.
[21] L.C. Bichara, H.E. Lanús, C.G. Nieto, S.A. Brandán, Density functional theory calculations of the molecular force field of L-ascorbic acid, vitamin C, J. Phys. Chem. 114 (2010) 4997–5004.
[22] A.B. Nielsen, A.J. Holder, Gauss View 5.0, User's Reference, GAUSSIAN Inc., Pittsburgh, PA, 2008.
[23] M.J. Frisch, G.W. Trucks, H.B. Schlegel, G.E. Scuseria, M.A. Robb, J.R. Cheeseman, G. Scalmani, V. Barone, B. Mennucci, G.A. Petersson, H. Nakatsuji, M. Caricato, X. Li, H.P. Hratchian, A.F. Izmaylov, J. Bloino, G. Zheng, J.L. Sonnenberg, M. Hada, M. Ehara, K. Toyota, R. Fukuda, J. Hasegawa, M. Ishida, T. Nakajima, Y. Honda, O. Kitao, H. Nakai, T. Vreven, J.A. Montgomery Jr., J.E. Peralta, F. Ogliaro, M. Bearpark, J.J. Heyd, E. Brothers, K.N. Kudin, V.N. Staroverov, R. Kobayashi, J. Normand, K. Raghavachari, A. Rendell, J.C. Burant, S.S. Iyengar, J. Tomasi, M. Cossi, N. Rega, J.M. Millam, M. Klene, J.E. Knox, J.B. Cross, V. Bakken, C. Adamo, J. Jaramillo, R. Gomperts, R.E. Stratmann, O. Yazyev, A.J. Austin, R. Cammi, C. Pomelli, J.W. Ochterski, R.L. Martin, K. Morokuma, V.G. Zakrzewski, G.A. Voth, P. Salvador, J.J. Dannenberg, S. Dapprich, A.D. Daniels, O. Farkas, J.B. Foresman, J.V. Ortiz, J. Cioslowski, D.J. Fox, Gaussian, Inc., Wallingford CT, 2009.
[24] S. Miertus, E. Scrocco, J. Tomasi, Electrostatic interaction of a solute with a continuum, Chem. Phys. 55 (1981) 117–129.
[25] J. Tomasi, J. Persico, Molecular interactions in solution: an overview of methods based on continous distributions of the solvent, Chem. Rev. 94 (1994) 2027–2094.
[26] A.V. Marenich, C.J. Cramer, D.G. Truhlar, Universal solvation model based on solute electron density and a continuum model of the solvent defined by the bulk dielectric constant and atomic surface tensions, J. Phys. Chem. B113 (2009) 6378–6396.
[27] B.H. Besler, K.M. Merz Jr., P.A. Kollman, Atomic charges derived from demi-empirical methods, J. Comput. Chem. 11 (1990) 431–439.
[28] E.D. Glendening, J.K. Badenhoop, A.D. Reed, J.E. Carpenter, F. Weinhold, NBO 3.1, Theoretical Chemistry Institute, University of Wisconsin, Madison, WI, 1996.
[29] R.F.W. Bader, Atoms in Molecules, A Quantum Theory, Oxford University Press, Oxford, 1990, ISBN 0198558651.
[30] F. Biegler-Köning, J. Schönbohm, D. Bayles, AIM2000; A program to analyze and visualize atoms in molecules, J. Comput. Chem. 22 (2001) 545.
[31] D. Romani, S.A. Brandán, Structural, electronic and vibrational studies of two 1,3-benzothiazole tautomers with potential antimicrobial activity in aqueous and organic solvents, Prediction of their reactivities, Computational and Theoretical Chem. 1061 (2015) 89–99.
[32] D. Romani, O. Noureddine, N. Issaoui, S.A. Brandán, Properties and reactivities of niclosamide in different media, a potential antiviral to treatment of COVID-19 by using DFT calculations and molecular docking, Biointerface Res. Appl. Chem 10 (6) (2020) 7295–7328.
[33] P. Ugliengo, MOLDRAW Program, University of Torino, Dipartimento Chimica IFM, Torino, Italy, 1998.
[34] S.A. Brandán, Why morphine is a molecule chemically powerful. Their comparison with cocaine, Indian J. Appl. Res. 7 (7) (2017) 511–528.
[35] S.A. Brandán, Understanding the potency of heroin against to morphine and cocaine, IJSRM, Int. J. Soc. Res. Methodol. 12 (2) (2018) 97–140.
[36] J. Hvoslef, The crystal structure of L-ascorbic acid, 'vitamin C'. II. The neutron diffraction analysis, Acta Crystallogr. B24 (1968) 1431.
[37] J. Hvoslef, The crystal structure of L-ascorbic acid, 'vitamin C'. I. The X-ray analysis, Acta Crystallogr. B24 (1968) 23.
[38] D.F. Veber, S.R. Johnson, H.-Y. Cheng, R. Brian, K.W. Ward, K.D. Kopple, Molecular Properties that influence the oral bioavailability of drug candidates, J. Med. Chem. 45 (2002) 2615–2623.
[39] C.A. Lipinski, F. Lombardo, B.W. Dominy, P.J. Feeney, Experimental and computational approaches to estimate solubility and permeability in drug discovery and development setting, Adv. Drug Deliv. Rev. 46 (2001) 3–26.
[40] J. Xu, P.-Y. Shi, H. Li, J. Zhou, Broad spectrum antiviral agent niclosamide and its therapeutic potential, ACS Infect. Dis. 6 (5) (2020) 909–915, https://doi.org/10.1021/acsinfecdis.0c00052.
[41] D. Romani, S.A. Brandán, Effect of the side chain on the properties from cidofovir to brincidofovir, an experimental antiviral drug against to Ebola virus disease, Arabian Journal of Chemistry 12 (2019) 2959–2972.
[42] a) G. Rauhut, P. Pulay, Transferable scaling factors for density functional derived vibrational force fields, J. Phys. Chem. 99 (1995) 3093–3099;
b) G. Rauhut, P. Pulay, J. Phys. Chem. 99 (1995) 14572.
[43] G. Keresztury, S. Holly, G. Besenyei, J. Varga, A.Y. Wang, J.R. Durig, Vibrational spectra of monothiocarbamates-II. IR and Raman spectra, vibrational assignment, conformational analysis and ab initio calculations of S-methyl-N,N-dimethylthiocarbamate Spectrochim, Acta 49A (1993) 2007–2026.
[44] D. Michalska, R. Wysokinski, The prediction of Raman spectra of platinum(II) anticancer drugs by density functional theory, Chem. Phys. Lett. 403 (2005) 211–217.
[45] T.J. Bruno, P.D.N. Svoronos, CRC Handbook of Basic Tables for Chemical Analysis, second ed., CRC Press, Taylor & Francis Goup, Boca Raton, 2011.
[46] R.A. Friedel, M. Orchin, Ultraviolet Spectra of Aromatic Compounds, Wiley & Sons, New York and London, 1951.